Letters

Highly Flexible and Mechanically Robust Ultrathin Au Grid as Electrodes for Flexible Organic Light-Emitting Devices

Fang-Shun Yi, Yan-Gang Bi, Xu-Lin Zhang, Da Yin, Yue-Feng Liu, Jing Feng, and Hong-Bo Sun, *Fellow, IEEE*

***Abstract*—We report a highly flexible ultrathin Au grid with high mechanical robustness as transparent electrode for flexible organic light-emitting devices (OLEDs). The grids are introduced to an ultrathin Au film to improve its optical transmittance and mechanical performance. With the line width of 15 μm and the gap width of 30 μm, the optimal ultrathin Au grid presents a desirable transmittance of 88.7% at 550 nm and a sheet resistance of 36 Ω/sq. Owing to the reduced tensile stress by the ultrathin grid patterns, the flexible ultrathin Au grid exhibits extraordinary mechanical stability with maintained conductivity after 48 000 bending cycles under a bending radius of 1 mm. Flexible OLEDs with high flexibility and mechanical robustness have been obtained using the ultrathin Au grid as the transparent anode by maintaining 92% initial efficiency after 4200 bending cycles. Moreover, flexible OLEDs exhibit a significantly improved current efficiency in comparison to the devices based on the continuous Au or traditional ITO anode.**

***Index Terms*—Ultrathin Au grid film, flexible transparent electrodes, mechanical robustness, flexible organic light-emitting devices.**

I. Introduction

FLEXIBLE organic light-emitting devices (OLEDs) have attracted great research interests owing to their availability in flat panel displays, mobile screens and wearable equipments [1]–[7]. Transparent conductive electrodes (TCEs) with excellent optical transparency and electrical conductivity, which act as the window for charge injection and photon extraction, play an important role in the performance of OLEDs [8]–[11]. In addition, owing to the promising applications of TCEs in flexible and wearable devices, flexibility and mechanical stability are further required. Indium tin oxide (ITO) is the most commonly used TCE in OLEDs [12], [13]. However, ITO suffers from several significant limitations as the flexible TCE, such as its brittleness with poor mechanical performance [14]–[17], the rising cost, and the incompatibility with plastic substrate due to the high processing temperature [18]–[20]. To satisfy the requirements of flexible applications, great endeavors have been dedicated to the development of novel flexible TCEs, including graphene [21]–[23], carbon nanotubes [24], [25], conducting polymers [26]–[28], metal nanowires [29]–[31], metal nanomesh [32]–[40] and ultrathin metal films [41], [42]. Recently, ultrathin and continuous metal films, with thickness below 10 nm, have leaded the way as the promising alternatives of ITO in flexible optoelectronic devices because of their low-cost manufacturing, mechanical flexibility, and high conductivity [4]. The work functions can be easily tuned as well by using different metallic materials. However, owing to the metallic absorption and reflection, the optical transparency of ultrathin metal films in the whole visible wavelength region is still lower and narrower than that of ITO, and it is limited to improve their optical properties by reducing the thickness of metal film. On the other hand, the formation and propagation of cracks in metal films during repeated bending dramatically break the optoelectronic performances of metal-based TCEs, resulting in an inferior mechanical stability.

In this letter, we propose a simple and low-cost method to realize an ultrathin Au grid film with desirable optoelectronic and mechanical performances. In the ultrathin Au grid film, a MoO_3-seeding-layer is used to suppress the Volmer–Weber growth mode of thermally deposited ultrathin Au film, and the periodic grids are introduced by lithography and wet-etching technologies. High and tunable optoelectronic characteristics of the ultrathin Au grid films are achieved by tuning the line width and spacing of the grid patterns [43]. The grid patterns can reduce the tensile stress during the bending cycles, which prevents Au film from cracking and the cracks propagating [44]. As a result, flexible OLEDs based on the ultrathin Au grid electrodes exhibit superior performance with higher efficiency and mechanical robustness, compared to the devices based on continuous Au

Manuscript received May 15, 2019; revised July 7, 2019; accepted July 10, 2019. Date of publication July 19, 2019; date of current version August 7, 2019. This work was supported in part by the National Key Research and Development Program of China and National Natural Science Foundation of China (NSFC) under Grants 2017YFB0404500, 61705075, 61825402, 61675085 and 61605056, and in part by the China Postdoctoral Science Foundation under Grant 2016M600230. The review of this letter was arranged by associate editor G.-B. Lee.

F.-S. Yi, Y.-G. Bi, X.-L. Zhang, D. Yin, Y.-F. Liu, and J. Feng are with the State Key Lab of Integrated Optoelectronics, College of Electronic Science and Engineering, Jilin University, Changchun 130012, China (e-mail: yangang_bi@jlu.edu.cn).

H.-B. Sun is with the State Key Lab of Integrated Optoelectronics, College of Electronic Science and Engineering, Jilin University, Changchun 130012, China, and also with the State Key Lab of Precision Measurement Technology and Instruments, Department of Precision Instrument, Tsinghua University, Beijing 100084, China (e-mail: hbsun@tsinghua.edu.cn).

This letter has supplementary downloadable material available at http://ieeexplore.ieee.org, provided by the authors.

Digital Object Identifier 10.1109/TNANO.2019.2928689

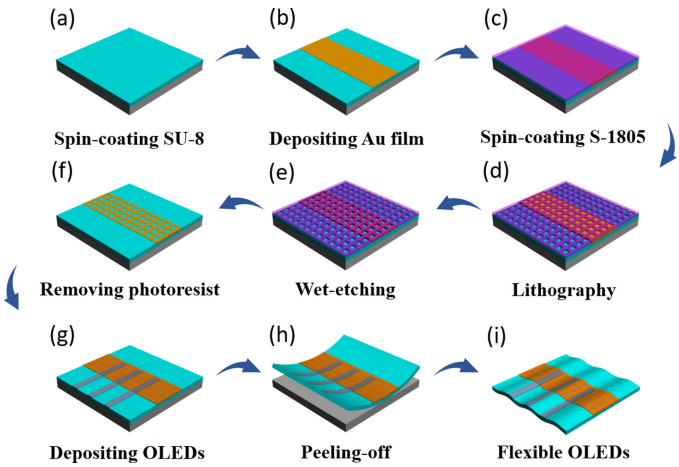

Fig. 1. Schematic of the fabrication process of the flexible OLEDs based on ultrathin Au grid electrodes by lithography and wet etching.

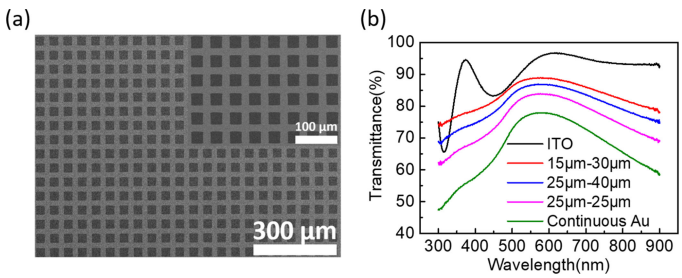

Fig. 2. (a) SEM image of 8 nm Au grid film with line width of 15 μm and gap width of 30 μm deposited on the glass substrate. (b) Transmittance spectra of ITO (black line), continuous Au film (8 nm, green line), and Au grid films (8 nm) with different line widths and gap widths. The line widths of the grid films are 15 μm (red line), 25 μm (blue line), 25 μm (pink line), respectively, and their gap widths are 30 μm, 40 μm, 25 μm, respectively.

electrodes and ITO electrodes, and remain 92% initial efficiency after 4200 bending cycles under a bending radius of 2 mm.

II. Experiment

A. Fabrication of the Ultrathin Au Grid Electrodes

The ultrathin Au grid films were prepared by thermally deposition, lithography, and wet-etching technologies as shown in Fig. 1. The glass substrates were cleaned successively with acetone, ethanol, deionized water and placed in a drying oven at 95 °C for 5 min. Then 3 nm MoO_3 and 8 nm Au were deposited on the cleaned substrates with a rate of 0.4 Å s^{-1} by physical vapor deposition. MoO_3 serves on a seeding layer to enhance the adhesion between the Au film and the substrate, and improve the surface appearance of the ultrathin Au film. The S-1805 photoresist (Rohm and Haas Electronic Materials, LLC) was spin-coated on the Au film at 1000 rpm for 1 min, and then baked in a drying oven at 95 °C for 3 min. Subsequently, the samples with various grid masks were exposed under an UV light for 50 s and developed for 5 s. The Au films were etched by etchant (0.2g KI + 0.05g I_2 + 10ml H_2O) [45] for 5 s. Finally, the samples were dipped in acetone for 15 s to remove the residual photoresist.

B. Fabrication of OLEDs

OLEDs were prepared based on ultrathin Au grid electrodes, continuous Au electrodes, and ITO electrodes, respectively. 3 nm MoO_3 was first deposited as an anode modification layer, followed by 40 nm N,N'-Diphenyl-N,N'-bis(1,1'-biphenyl)-4,4'-diamine (NPB) as a hole transporting layer. 4,4'-Bis(N-carbazolyl)-1,1'-biphenyl (CBP) doped with 5 wt% of phosphorescent emitter 2,3,5,6-tetrakis(3,6-diphenylcarbazol-9-yl)-1,4-dicyanobenzene ($Ir(BT)_2(acac)$) were co-deposited as the orange light-emitting layer with the thickness of 30 nm. Finally, 20 nm 2,2',2"(1,3,5-Nbenzenetriyl)tris-[1-phenyl-1H-benzimidazole] (TpBi) as an electron transporting layer, 3 nm Ca and 80 nm Ag as the cathode were deposited, respectively. The structures of the OLEDs are glass substrate/anode (Au grid/continuous Au/ITO)/MoO_3/NPB/CBP: $Ir(BT)_2(acac)$/TpBi/Ca/Ag.

C. Fabrication of Flexible OLEDs

The glass substrate was treated with Octadecyltrichlorosilane (OTS) for 10 h in a drying oven at 95 °C. Then an ultrathin layer of SU-8 2025 (MicroChem Corp.) was spin-coated at 4500 rpm and was exposed for 2 min under UV light, which acted as a flexible substrate (Fig. 1(a)). After the fabrication of various anodes and OLEDs, the flexible OLEDs deposited on the SU-8 2025 film were peeled off from the glass substrates (Fig. 1(h) and 1(i)).

D. Characterizations of Electrodes and OLEDs

The surface morphologies of the ultrathin Au grid films were characterized by a scanning electron microscope (SEM, JSM-7500F, JEOL) and an atomic force microscope (AFM, Icon, Bruker). The sheet resistance was measured by a four-point probe system (RTS-5, PROBES TECH), and a UV-Vis spectrophotometer (UV-2550, SHIMADZU) was used to measure the transmittance. The electroluminescence (EL) performance of OLEDs was measured by a PR655 spectroradiometer (Photo Research Inc.) and a Keithley 2400 Source.

III. Results and Discussions

The surface morphologies of our proposed ultrathin Au grid films were characterized by SEM as shown in Fig. 2(a) and Fig. S2. The ultrathin Au grid films demonstrate uniformity of the patterns with a very little error compared with the designed parameters over a large area, and clear boundaries without residual photoresist. The optical transparency and electrical conductivity of the ultrathin Au grid films are determined by the line widths and gap widths of the grid patterns [43]. The dependences of the transmittance and sheet resistance of the ultrathin Au grid films on the line widths and gap widths are summarized in Fig. 2(b) and Table I. The optoelectronic properties of continuous ultrathin Au films and ITO were also measured for comparison. In the measurement of optical transparency, the influence of glass substrate has been deducted by using a bare glass as a reference. The 8 nm continuous Au film with a transmittance of 77.4% at 550 nm has been achieved, which is

TABLE I
TRANSMITTANCE, SHEET RESISTANCE (R_s), AND FIGURE OF MERIT (FOM) OF TRANSPARENT CONDUCTIVE FILMS

line width - gap width	T (%)	R_s (Ω/sq)	FOM (x10^{-3} Ω^{-1})
Continuous Au	77.409	15	5.15
15μm-30μm	88.651	36	8.33
25μm-40μm	86.555	29	8.14
25μm-25μm	83.469	21	7.82

T (%) is the transmittance at 550 nm.

much lower and narrower than that of ITO (93.6% @550 nm). After introducing the grid patterns, the ultrathin Au films demonstrate high and broad optical transparent properties, and the transmittance of the ultrathin Au grid film with the line width of 25 μm and the gap width of 25 μm is 83.5% at 550 nm. The optical performance of ultrathin Au grid films can be further improved by decreasing the line widths and increasing the gap widths of the grid patterns. The 8 nm ultrathin Au grid film with 15 μm line width and 30 μm gap width exhibits a uniform and high transmittance of 88.7% @550 nm. However, the grid patterns reduce the effective area of the electrical conductor, which leads to the degeneration in conductivity. As summarized in Table I, the sheet resistances of ultrathin Au grid films with various line widths and gap widths are increased to 36 Ω/sq, 29 Ω/sq, and 21 Ω/sq, respectively, compared to the continuous Au film with sheet resistance of 15 Ω/sq.

The figure of merit (FOM) is usually introduced [46] to evaluate the optoelectronic characteristics of transparent conductive film which is defined by the Haacke equation:

$$\mathrm{FOM} = \frac{T^{10}}{R_s} \tag{1}$$

in which T represents the visible light transmittance (@550 nm), and R_s represents the sheet resistance. Table I shows the calculated FOMs of ultrathin continuous Au film and ultrathin Au grid films based on 8 nm-thickness Au. The ultrathin Au grid film with line width of 15 μm and gap width of 30 μm shows a superior FOM, and as a result, it is applied as the transparent anode in rigid and flexible OLEDs.

The inset in Fig. 3(a) shows the schematic structure of flexible OLEDs based on the ultrathin Au grid anode, and OLEDs based on continuous Au anode and ITO anode were also prepared as reference. The performances of OLEDs are summarized in Fig. 3. The maximum luminance of flexible OLEDs and rigid OLEDs based on ultrathin Au grid anode is 41710 cd/m^2 and 42930 cd/m^2, respectively, while the maximum luminance of planar rigid OLEDs based on continuous Au anode and ITO anode is 64690 cd/m^2 and 68480 cd/m^2, respectively (Fig. 3(a)). The decrease in luminance of OLEDs based on grid electrode is caused by the reduced effective light-emitting area in the grid patterns, in which the non-conductive spacing regions cannot emit light, as shown in Fig. 3(e) and Fig. 3(f). The non-conductive spacing gaps also decrease the current density of the grid-electrode-based OLEDs (Fig. 3(b). However, in the calculation of current efficiency of OLEDs, the mismatch in

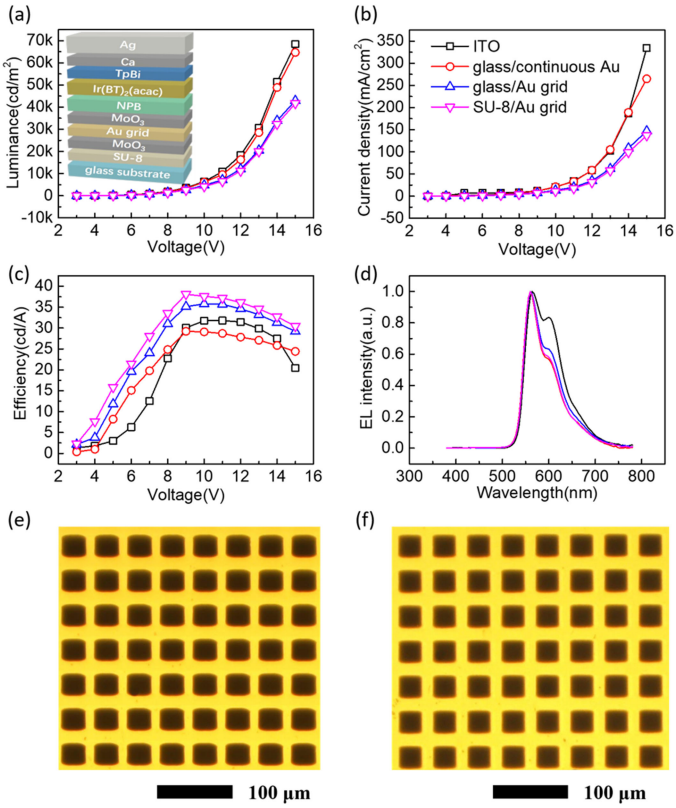

Fig. 3. EL performance of the OLEDs. (a) Luminance-voltage, (b) current density-voltage, (c) efficiency-voltage and (d) normalized EL spectra of OLEDs based on the SU-8/Au grid anode (flexible OLEDs), glass/Au grid anode (rigid OLEDs), glass/continuous Au anode (rigid OLEDs), ITO anode (rigid OLEDs). The inset in (a) shows the schematic structure of flexible OLEDs based on the ultrathin Au grid anode. The optical microscope images of working OLEDs based on glass/Au grid anode and SU-8/Au grid anode are shown in (e) and (f), respectively.

effective area between continuous-electrode-based devices and grid-electrode-based devices can be eliminated. As shown in Fig. 3(c), the maximum efficiency of flexible OLEDs with ultrathin Au grid anode is 38.1 cd/A and the maximum efficiency of rigid OLEDs with ultrathin Au grid anode is 35.8 cd/A, which are significantly higher than those of the continuous-Au-anode-based OLEDs (29.2 cd/A) and the ITO-anode-based OLEDs (31.8 cd/A). Owing to the improved transmittance in the whole visible wavelength by the grid patterns, we obtain a 30% improvement in current efficiency from the OLEDs based on ultrathin Au grid anode. Owing to the high refractive index of ITO, the light can be reflected at the interface between ITO and glass substrate, which, leads to the power loss in the waveguide mode in ITO-based OLEDs [47], [48]. Although the transparency of ultrathin Au grid electrode is slightly lower than that of ITO, the superior performances in grid-electrode-based OLEDs are still achieved due to the suppression of ITO induced waveguide mode [4].

The flexibility and mechanical stability of the ultrathin Au grid electrode and OLEDs have been evaluated by bending tests. After 48,000 bending cycles with a bending radius of only 1 mm, continuous Au electrode exhibits a 38% increasement in sheet resistance. While the ultrathin Au grid electrode demonstrates

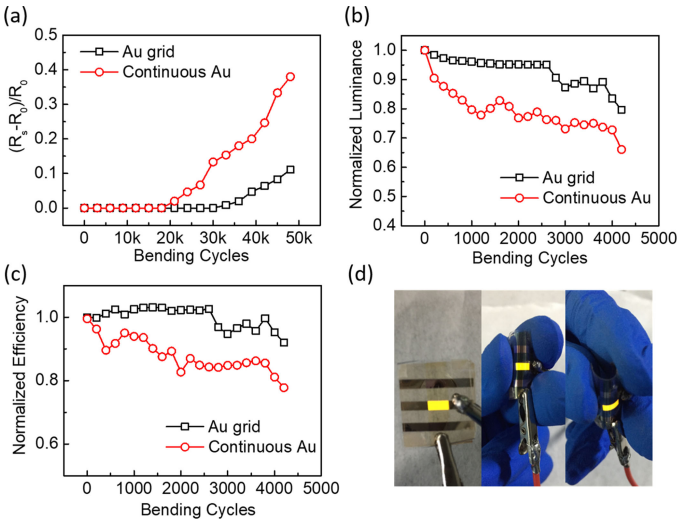

Fig. 4. Flexibility and mechanical stability of the flexible electrodes and flexible OLEDs. (a) The sheet resistances of the 8 nm flexible ultrathin Au grid electrode and continuous Au electrode as a function of bending cycles. R_o and R_s represent the sheet resistance before and after bending, respectively. (b) Normalized luminance and (c) normalized current efficiency of the OLEDs at 6 V as a function of bending cycles. (d) The photographs of the flexible OLEDs operated at 6 V before and after bending.

the more striking mechanical stability with a mere 11% increase in sheet resistance (Fig. 4(a)) which is at the forefront of many reported flexible TCEs [49]–[51]. In addition to photolithography [36], there are many other techniques to achieve gold meshes, such as self-assembly [32]–[34], electron beam lithography [37], nanosphere lithography [38], grain boundary lithography [39], and template method with sacrificial layers [40]. We have compared the performance of the 8 nm ultrathin Au grid film with them in Table S1, and our proposed ultrathin Au grid electrode shows excellent flexibility and mechanical stability. The superior mechanical stability of the ultrathin Au grid electrode, compared to the continuous Au electrode, arises from the grid patterns which can reduce the tensile stress during the bending cycles to prevent Au film from cracking and stop the cracks propagating. On the other hand, the mechanical stability of ultrathin metal film is usually better than that of thick metal film. Although the 30 nm Au grid electrode (6 Ω/sq) and the continuous Au electrode (2 Ω/sq) have excellent conductivity, they turn to be nonconductive after 800 bending cycles and 600 bending cycles, respectively, as shown in Fig. S4. The strong adhesion between Au grid and the substrate is demonstrated by tape adhesion test, which is conducted by a 3M Scotch tape. As shown in Fig. S5, the ultrathin Au grid film fabricated by lithography and wet-etching maintained its conductivity after 50 taping cycles, demonstrating its high durability against mechanical delamination from the substrate. Figs. 4(b) and (c) show the luminance and efficiency of the OLEDs based on 8 nm ultrathin Au grid electrode and continuous Au electrode in the bending test. After 4200 bending cycles under a bending radius of 2 mm, the flexible OLEDs based on continuous Au electrode remain only 66% of initial luminance and 78% of initial efficiency. However, the luminance and efficiency of flexible OLEDs based on ultrathin Au grid electrode maintain 80% and 92% of their initial values respectively under the same bending conditions, demonstrating the high flexibility and mechanical robustness.

IV. Conclusions

In summary, we fabricated an 8 nm ultrathin Au grid electrode by a simple method as the replacement of ITO in flexible OLEDs. The ultrathin Au grid electrode demonstrates desirable and broad optical transparent properties, with the transmittance of 88.7% at 550 nm, and high electrical conductivity, with the sheet resistance of 36 Ω/sq. Owing to the excellent optoelectrical properties of the ultrathin Au grid electrode, we obtain a considerable enhancement in current efficiency of the ultrathin Au grid electrode-based OLEDs compared to that of the continuous Au electrode-based and traditional ITO electrode-based OLEDs. Moreover, the ultrathin Au grid electrode exhibits outstanding flexibility and mechanical robustness due to the reduced tensile stress by grid patterns during the bending cycles. 89% initial conductivity of the ultrathin Au grid electrode and 92% initial efficiency of the flexible OLEDs are remained after 48000 and 4200 bending cycles, respectively. The ultrathin Au grid electrode is undoubtedly promising for the application of flexible devices in wearable equipments.

References

[1] H. W. Chen, J. H. Lee, B. Y. Lin, S. Chen, and S. T. Wu, "Liquid crystal display and organic light-emitting diode display: Present status and future perspectives," *Light Sci. Appl.*, vol. 7, Mar. 2018, Art. no. 17168.
[2] J. Feng, Y. F. Liu, Y. G. Bi, and H. B. Sun, "Light manipulation in organic light-emitting devices by integrating micro/nano patterns," *Laser Photon. Rev.*, vol. 11, no. 2, Mar. 2017, Art. no. 1600145.
[3] F. Guo, A. Karl, Q. F. Xue, K. C. Tam, K. Forberich, and C. J. Brabec, "The fabrication of color-tunable organic light-emitting diode displays via solution processing," *Light Sci. Appl.*, vol. 6, Nov. 2017, Art. no. e17094.
[4] Y. G. Bi *et al.*, "Ultrathin and ultrasmooth Au films as transparent electrodes in ITO-free organic light-emitting devices," *Nanoscale*, vol. 8, no. 19, pp. 10010–10015, 2016.
[5] R. Ding *et al.*, "Highly efficient three primary color organic single-crystal light-emitting devices with balanced carrier injection and transport," *Adv. Funct. Mater.*, vol. 27, no. 13, Apr. 2017, Art. no. 1604659.
[6] D. Yin *et al.*, "Mechanically robust stretchable organic optoelectronic devices built using a simple and universal stencil-pattern transferring technology," *Light Sci. Appl.*, vol. 7, Jul. 2018, Art. no. 35.
[7] G. J. Liang *et al.*, "Self-healable electroluminescent devices," *Light Sci. Appl.*, vol. 7, Dec. 2018, Art. no. 102.
[8] A. Aliprandi *et al.*, "Hybrid copper-nanowire-reduced-graphene-oxide coatings: A "green solution" toward highly transparent, highly conductive, and flexible electrodes for (Opto) electronics," *Adv. Mater.*, vol. 29, no. 41, Nov. 2017, Art. no. 1703225.
[9] M. Morales-Masis, S. De Wolf, R. Woods-Robinson, J. W. Ager, and C. Ballif, "Transparent Electrodes for Efficient Optoelectronics," *Adv. Electron. Mater.*, vol. 3, no. 5, May 2017, Art. no. 1600529.
[10] J. Yang, C. X. Bao, K. Zhu, T. Yu, and Q. Y. Xu, "High-performance transparent conducting metal network electrodes for Perovksite photodetectors," *ACS Appl. Mater. Interfaces*, vol. 10, no. 2, pp. 1996–2003, Jan. 2018.
[11] E. Lee *et al.*, "All-solution-processed silver nanowire window electrode-based flexible perovskite solar cells enabled with amorphous metal oxide protection," *Adv. Energy Mater.*, vol. 8, no. 9, Mar. 2018, Art. no. 1702182.
[12] S. Kee *et al.*, "Highly deformable and see-through polymer light-emitting diodes with all-conducting-polymer electrodes," *Adv. Mater.*, vol. 30, no. 3, Jan. 2018, Art. no. 1703437.
[13] Y. H. Chen *et al.*, "Organic semiconductor heterojunctions: Electrode-independent charge injectors for high-performance organic light-emitting diodes," *Light Sci. Appl.*, vol. 5, Mar. 2016, Art. no. e16042.

[14] V. Reboud *et al.*, "Enhanced light extraction in ITO-free OLEDs using double-sided printed electrodes," *Nanoscale*, vol. 4, no. 11, pp. 3495–3500, 2012.

[15] S. Schubert, M. Hermenau, J. Meiss, L. Muller-Meskamp, and K. Leo, "Oxide sandwiched metal thin-film electrodes for long-term stable organic solar cells," *Adv. Funct. Mater.*, vol. 22, no. 23, pp. 4993–4999, Dec. 2012.

[16] C. Zhang *et al.*, "An ultrathin, smooth, and low-loss al-doped Ag film and its application as a transparent electrode in organic photovoltaics," *Adv. Mater.*, vol. 26, no. 32, pp. 5696–5701, Aug. 2014.

[17] Y. S. Oh *et al.*, "Temperature-controlled direct imprinting of Ag ionic ink: Flexible metal grid transparent conductors with enhanced electromechanical durability," *Sci. Rep.*, vol. 7, Sep. 2017, Art. no. 11220.

[18] H. M. Stec, R. J. Williams, T. S. Jones, and R. A. Hatton, "Ultrathin transparent au electrodes for organic photovoltaics fabricated using a mixed mono-molecular nucleation layer," *Adv. Funct. Mater.*, vol. 21, no. 9, pp. 1709–1716, May 2011.

[19] S. Schubert, J. Meiss, L. Muller-Meskamp, and K. Leo, "Improvement of transparent metal top electrodes for organic solar cells by introducing a high surface energy seed layer," *Adv. Energy Mater.*, vol. 3, no. 4, pp. 438–443, Apr. 2013.

[20] J. Y. Zou, C. Z. Li, C. Y. Chang, H. L. Yip, and A. K. Y. Jen, "Interfacial engineering of ultrathin metal film transparent electrode for flexible organic photovoltaic cells," *Adv. Mater.*, vol. 26, no. 22, pp. 3618–3623, Jun. 2014.

[21] T. H. Han *et al.*, "Extremely efficient flexible organic light-emitting diodes with modified graphene anode," *Nature Photon.*, vol. 6, no. 2, pp. 105–110, Feb. 2012.

[22] Y. Chen *et al.*, "Microscale-patterned graphene electrodes for organic light-emitting devices by a simple patterning strategy," *Adv. Opt. Mater.*, vol. 6, no. 13, Jul. 2018, Art. no. 1701348.

[23] L. Wang *et al.*, "Broadband tunable liquid crystal terahertz waveplates driven with porous graphene electrodes," *Light Sci. Appl.*, vol. 4, Feb. 2015, Art. no. e253.

[24] J. Li, L. Hu, L. Wang, Y. Zhou, G. Gruner, and T. J. Marks, "Organic light-emitting diodes having carbon nanotube anodes," *Nano Lett.*, vol. 6, no. 11, pp. 2472–2477, Nov. 8. 2006.

[25] D. Zhang *et al.*, "Transparent, conductive, and flexible carbon nanotube films and their application in organic light-emitting diodes," *Nano Lett.*, vol. 6, no. 9, pp. 1880–1886, Sep. 13, 2006.

[26] H.-W. Chang *et al.*, "Color-stable, ITO-free white organic light-emitting diodes with enhanced efficiency using solution-processed transparent electrodes and optical outcoupling layers," *Org. Electron.*, vol. 15, no. 5, pp. 1028–1034, May 2014.

[27] M. Jiao, C.-Y. Lu, W.-K. Lee, C.-Y. Chen, and C.-C. Wu, "Simple planar indium-tin-oxide-free organic light-emitting devices with nearly 39% external quantum efficiency," *Adv. Optical Mater.*, vol. 4, no. 3, pp. 365–370, Mar. 2016.

[28] P. Matyba, H. Yamaguchi, G. Eda, M. Chhowalla, L. Edman, and N. D. Robinson, "Graphene and mobile ions: The key to all-plastic, solution-processed light-emitting devices," *ACS Nano*, vol. 4, no. 2, pp. 637–642, Feb. 2010.

[29] H. Wu *et al.*, "A transparent electrode based on a metal nanotrough network," *Nature Nanotechnol.*, vol. 8, no. 6, pp. 421–425, Jun. 2013.

[30] J. Park *et al.*, "Flexible transparent conductive films with high performance and reliability using hybrid structures of continuous metal nanofiber networks for flexible optoelectronics," *ACS Appl. Mater. Interfaces*, vol. 9, no. 24, pp. 20299–20305, Jun. 2017.

[31] L. Lian, D. Dong, D. X. Feng, and G. F. He, "Low roughness silver nanowire flexible transparent electrode by low temperature solution-processing for organic light emitting diodes," *Org. Electron.*, vol. 49, pp. 9–18, Oct. 2017.

[32] M. D. Ho, Y. Y. Liu, D. S. Dong, Y. M. Zhao, and W. L. Cheng, "Fractal gold nanoframework for highly stretchable transparent strain-insensitive conductors," *Nano Lett.*, vol. 18, no. 6, pp. 3593–3599, Jun. 2018.

[33] Y. Wang *et al.*, "Self-assembled gold nanorime mesh conductors for invisible stretchable supercapacitors," *Nanoscale*, vol. 10, no. 34, pp. 15948–15955, Sep. 2018.

[34] S. Gong *et al.*, "Fabrication of highly transparent and flexible nanomesh electrode via self-assembly of ultrathin gold nanowires," *Adv. Electron. Mater.*, vol. 2, no. 7, Jul. 2016, Art. no. 1600121.

[35] B. W. Zhu, S. Gong, and W. L. Cheng, "Softening gold for elastronics," *Chem. Soc. Rev.*, vol. 48, no. 6, pp. 1668–1711, Mar. 2019.

[36] F. L. M. Sam, C. A. Mills, L. J. Rozanski, and S. R. P. Silva, "Thin film hexagonal gold grids as transparent conducting electrodes in organic light emitting diodes," *Laser Photon. Rev.*, vol. 8, no. 1, pp. 172–179, Jan. 2014.

[37] G. H. Yang, B. Liu, K. Cheng, and Z. L. Du, "Modulation of optical transmittance and conductivity by the period, linewidth and height of Au square mesh electrodes," *Opt. Express*, vol. 23, no. 3, pp. A62–A70, Feb. 2015.

[38] Z. P. Li, G. Wang, Z. M. Li, Z. Z. Cheng, G. P. Zhou, and S. Li, "Flexible transparent electrodes based on gold nanomeshes," *Nanoscale Res. Lett.*, vol. 14, Apr. 2019, Art. no. 132.

[39] C. F. Guo, T. Y. Sun, Q. H. Liu, Z. G. Suo, and Z. F. Ren, "Highly stretchable and transparent nanomesh electrodes made by grain boundary lithography," *Nature Commun.*, vol. 5, Jan. 2014, Art. no. 3121.

[40] K. J. Seo *et al.*, "Wafer-scale, stretchable nanomeshes from an ultrathin-support-layer assisted transfer," *Appl. Phys. Lett.*, vol. 112, no. 26, Jun. 2018, Art. no. 263101.

[41] L. Vj *et al.*, "Ultrasmooth silver thin films deposited with a germanium nucleation layer," *Nano Lett.*, vol. 9, no. 1, pp. 178–182, Jan. 2009.

[42] N. Formica, D. S. Ghosh, A. Carrilero, T. L. Chen, R. E. Simpson, and V. Pruneri, "Ultrastable and atomically smooth ultrathin silver films grown on a copper seed layer," *ACS Appl. Mater. Interfaces*, vol. 5, no. 8, pp. 3048–3053, Apr. 2013.

[43] L. Zhou *et al.*, "Screen-printed poly(3,4-ethylenedioxythiophene): Poly(styrenesulfonate) grids as ITO-free anodes for flexible organic light-emitting diodes," *Adv. Funct. Mater.*, vol. 28, no. 11, Mar. 2018, Art. no. 1705955.

[44] K. Sakamoto, H. Kuwae, N. Kobayashi, A. Nobori, S. Shoji, and J. Mizuno, "Highly flexible transparent electrodes based on mesh-patterned rigid indium tin oxide," *Sci. Rep.*, vol. 8, Feb. 2018, Art. no. 2825.

[45] E. C. Cho, J. W. Xie, P. A. Wurm, and Y. N. Xia, "Understanding the role of surface charges in cellular adsorption versus internalization by selectively removing gold nanoparticles on the cell surface with a I-2/KI etchant," *Nano Lett.*, vol. 9, no. 3, pp. 1080–1084, Mar. 2009.

[46] G. Haacke, "New figure of merit for transparent conductors," *J. Appl. Phys.*, vol. 47, no. 9, pp. 4086–4089, 1976.

[47] K. Hong and J. L. Lee, "Review paper: Recent developments in light extraction technologies of organic light emitting diodes," *Electron. Mater. Lett.*, vol. 7, no. 2, pp. 77–91, Jun. 2011.

[48] C. M. Hsu, W. T. Wu, Y. X. Zeng, B. T. Lin, and W. M. Lin, "Organic light-emitting diodes fabricated on recessed anodes for light extraction enhancement," *Org. Electron.*, vol. 17, pp. 340–348, Feb. 2015.

[49] Z. Yin, C. Lee, S. Cho, J. Yoo, Y. Piao, and Y. S. Kim, "Facile synthesis of oxidation-resistant copper nanowires toward solution-processable, flexible, foldable, and free-standing electrodes," *Small*, vol. 10, no. 24, pp. 5047–5052, Dec. 2014.

[50] H. J. Lee *et al.*, "Effective indium-doped zinc oxide buffer layer on silver nanowires for electrically highly stable, flexible, transparent, and conductive composite electrodes," *ACS Appl. Mater. Interfaces*, vol. 5, no. 21, pp. 10397–10403, Nov. 2013.

[51] D. J. Kim, H. J. Kim, K. W. Seo, K. H. Kim, T. W. Kim, and H. K. Kim, "Indium-free, highly transparent, flexible $Cu_2O/Cu/Cu_2O$ mesh electrodes for flexible touch screen panels," *Sci. Rep.*, vol. 5, Nov. 2015, Art. no. 16838.